RSC Advances

ROYAL SOCIETY OF CHEMISTRY

www.rsc.org/advances

Cite this: DOI: 10.1039/c0xx00000x

www.rsc.org/xxxxxx

ARTICLE TYPE

T_1-weighted and T_2-weighted MRI probe based on Gd-DTPA surface conjugated SPIO nanomicelles

Waiou Zhao[b],Hailong Huang[a],Yuan Sun[a],Xiaonan Zhang[b],Yapeng Li[a],* and Jingyuan Wang[a]

[a]Alan G. MacDiarmid Institute of Jilin University, 2699 Qianjin Street, Changchun, China.

[b]The first hospital of Jilin University, Changchun, China

Herein we report a novel gadolinium chelate surface conjugated superparamagnetic iron oxide (SPIO) nanomicelles. In our design, Gd-diethylenetriaminepentaacetic acid(Gd-DTPA) conjugated with the folic acid (FA) targeting polyaspartic derivative (PASPD) coating surface of SPIO nanoparticles (IO-PASPD). The morphology of the Gd-DTPA-IO-PASPD was uniform spherical with an average particle size of 50 nm measured by dynamic light scattering (DLS) and transmission electron microscopy (TEM) imaging. The stability results showed that the FA-Gd-DTPA-IO-PASPD can stably preserve IO under physiological conditions (pH 7.4). An MTT assay showed that the cytotoxicity of FA-Gd-DTPA-IO-PASPD against hepatoma carcinoma (HepG2) cells was no significant after 24 h incubation. MRI in vitro and in vivo were also imaged and characterized. In summary, FA-Gd-DTPA-IO-PASPD could achieve T_1-weighted and T_2-weighted MR imaging stimultaneously and lengthen the half life time.

Introduction

Magnetic resonance imaging (MRI) has been recognized as a powerful noninvasive diagnostic technique to visualize the fine structure of human bodies in high spatial resolution, which results from perturbation of tissue water protons in the presence of external magnetic field.[1,2] MR contrast agent could create good images for diagnosis by shortening the longitudinal relaxation time (T_1) or the traverse relaxation time (T_2) of the surrounding water protons.[3,4] Paramagnetic gadolinium chelates which create an increase in T_1-weighted signal intensity (bright signal) have been demonstrated as a T_1-weighted contrast (positive contrast).[5] On the other hand, superparamagnetic iron oxide nanoparticles (SPIONPs) with polymeric coating which could decrease the T_2-weighted MR signal (dark signal) could be demonstrated as a T_2-weighted contrast (negative contrast).[6,7]

As we all know, gadolinium is often used clinically as a chelate, for example Gd-diethylenetriaminepentaacetic acid (DTPA) and Gd-1,4,7,10-tetraazacyclododecane-1,4,7,10-triacetic acid (DOTA).[8-10] However, the low-molecular weighted Gd chelates rapidly diffuse out of the blood following administration in the vein, resulting in a low half-life,[11-12] while the negative contrast showed a longer half-life in spite of the fact that iron oxide nanoparticles is often confused with a low-level MR signal arising from adjacent tissues such as bone or vasculature.[13-14] In order to improve the sensitivity and specificity of lesion detection, several studies of dual-contrast (DC) MR imaging involving the administration of SPIO and gadolinium chelates have been described.[15-16] Although this technique has been demonstrated to be able to improve the detection of hepatocellular carcinoma (HCC) nodules.[17-18] It is still restricted by the short detection time, resulting in a short half-life of gadolinium chelates.

To overcome the disadvantages above, dual-mode MR contrast prepared by gadolinium-encapsulating iron oxide has been designed and prepared.[19] The large magnetic moment of the iron oxide core would create a strong magnetic susceptibility in the proximity of the iron oxide core that will affect the T_1 relaxation of the Gd-DTPA encapsulated within the nanoparticle's polymeric coating. The quenching of T_1 signal made a failure in T_1-weighted imaging of the dual-mode MR contrast. Santra etc. have proved that the conjugation of Gd-DTPA directly on the nanoparticle's surface would not result in quenching of the T_1 values because of the further distance between Gd-DTPA and iron oxide core.[9] Therefore, an optimal dual-MR imaging contrast would be made by gadolinium chelate surface conjugated SPIO nanomicelles, to achieve T_1-weighted and T_2-weighted MR imaging stimultaneously and lengthen the half life time.

In this study, a new folic acid-targeted dual-mode MR contrast agent has been designed, synthesised and characterized. The designed MR agent is composed of Gd-DTPA surface conjugated the polyaspartic acid derivative (PASPD) coating of SPIO. The prepared dual-MR imaging contrast was carefully characterized and their stability, toxicity and paramagnetic relaxivity were evaluated. The T_1-weighted and T_2-weighted MRI in vivo were also evaluated.

Experimental

Materials

L-ASP (L-aspartic acid), diethylenetriaminepentaacetic acid (DTPA) dianhydride, gadolinium(Ⅲ) chloride hexahydrate, folic acid (FA), α-methoxy-ω-amino-poly(ethylene glycol) (Mn=2000)

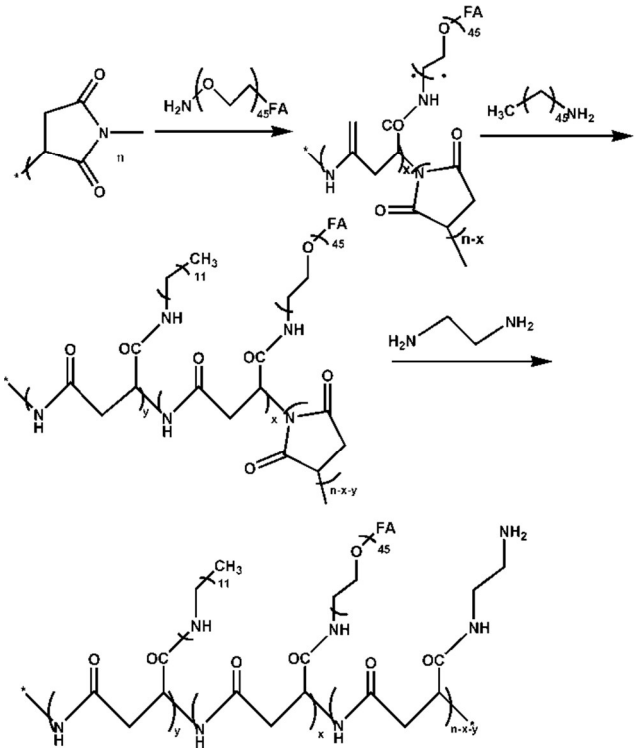

Scheme 1 The synthesis route for the polymer coating: PASP-g-(PEG-FA)-DDA-EDA

(MeO-PEG_{2000}-NH_2) and 1, ω-diaminopolyoxyethylene (H_2N-PEG_{2000}-NH_2) were obtained from the Adrich. 85% phosphoric acid, dodecylamine (DDA), Ethylenediamine (EDA) (Beijing Chemical works) were commercially available and used without further purification. N,N-dimethyl-formamide (DMF), dimethylsulfoxide (DMSO) were purchased from Beijing Chemical works (China) with further purification. A human liver cancer HepG2 cells was obtained from the second hospital of Jilin University (Changchun, China). 3-(4,5-dimethythiazol-2-yl)-2,5-diphenyltetrazolium bromide (MTT) from Beijing CellChip Biotechnology Co. Ltd. IONPs were purchased from Ocean NanoTech. (SOR-10, 10 nm, oleic acid coating). Male ICR mice (6-7 weeks old) were purchased from experimental animal center of Jilin University.

Characterization

The molecular weights and polydispersity of the polymers (Mw/Mn; Mw=weight-average molecular weight; Mn=number-average molecular weight) were recorded on a gel permeation chromatograph (GPC) equipped with two Mixed-B columns (pore size=10 μm; column size=300 × 7.5 mm) and refractive index detector (Perkin-ElmerSeries 200) using DMF (0.01 mol/L LiBr) as the eluent at 30 ℃ with a flow rate of 1 mL/min. The column system was calibrated by a set of mono-dispersed standard polystyrenes. ^{1}H-NMR spectra were obtained on a 500 Bruker NMR instrument using $CDCl_3$, DMSO-d_6 as the solvent and TMS as a reference standard for chemical shifts.

Hydrodynamic diameters (HD) and size distribution of polymer micelles and conjugate micelles were determined by dynamic light scattering (DLS) using a Brookheaven BI9000AT system Brookheaven Instruments Corporation, USA, with reproducibility verified by collection and comparison of sequential measurements. Shall model was chosen as the test mode. Measurements were performed at a 90° scattering angle at 25 °C. Each sample was measured in triplicate with 7 runs in each measurement and 90 s duration in each run. TEM imaging was used to show the size and the distribution of conjugate micelles (JEOL-2000, Japan). MTT assay was measured by BioTek Elx 800 at a wavelength of 490 nm. The Gd metal content was determined using an inductively coupled argon plasma optical emission spectrometer (ICP-OES) (Optima 3100XL, USA)

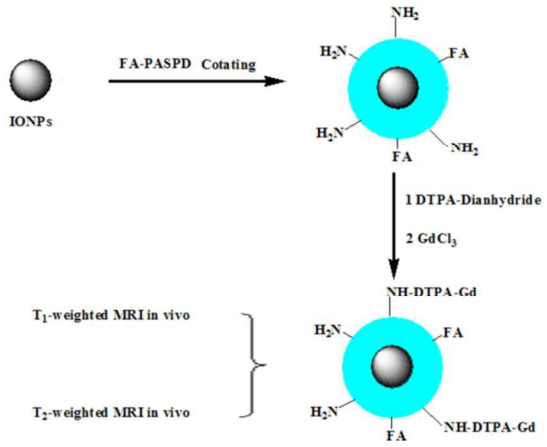

Scheme 2 A schematic illustration for the formation of Gd-DTPA-FA-PASPD-IO.

Synthesis and characterization of FA-PASPD@IO

The FA-PASPD which has hydrophilic segment and hydrophobic segment can be formed micelles easily. Hydrophobic-hydrophobic interaction between organic soluble IONPs and hydrophobic segments DDA of FA-PASPD makes IONPs water soluble. The novel IONPs can be used as MRI contrast agents. FA-PASPD (100 mg) was dissolved in 2 mL $CHCl_3$, 25 mg IONPs was dissolved in 2 mL $CHCl_3$, too. Deionized water (10 mL) was added drop by drop to the chloroform solution under ultrasonic wave. Chloroform was then gradually removed by rotary evaporation.

Synthesis and characterization of Gd-DTPA-FA-PASPD@IO

DTPA-dianhydride (71.6 mg, 0.2 mmol) was added in portions over a period of 30 min into a solution of FA-PASPD-IO (12.5 mg, ~ 0.046 mmol [NH_2]) in 2 mL of 0.1 M $NaHCO_3$. The pH of the reaction solution was adjusted to 8 by adding aliquots of 0.1 N NaOH solution. After being stirred at room temperature for 2 h, the reaction mixture was dialyzed against PBS and deionized water (MWCO 8000). The resulting solution was concentrated to 1 mL and stored at 4 ℃ for future use. The amount of DTPA attached to FA-PASPD-IO was determined by quantifying unreacted amino groups with the fluorescent amine method. Approximately 52% the amino groups in FA-PASPD were conjugated to DTPA.

To chelate with Gd^{3+}, a solution of $GdCl_3 \cdot 6H_2O$ in water (100 mg/mL) was added dropwise to the aqueous solution of DTPA-FA-PASPD-IO. The presence of trace amounts of unchelated Gd^{3+} in the mixture was monitored with a Gd^{3+} indicator 4-(2-pyridylazo) resorcinol. The reaction solution was dialyzed against

water (MWCO 8000) until no free gadolinium was detected in the receiving medium. The compound contained 16.7 % (w/w) of gadolinium as determined by elemental analysis. The obtained Gd-DTPA-FA-PASPD@IO (with molar ratio of Gd/Fe=0.25/1.00) were stored at 4 ℃ before use.

Table 1 Characterization results for all the nanoparticles

Nanoparticles	Dispersed in	Diameter		Fe content (mmol/mL)	Gd content (mmol/mL)
IO (oleic acid coating)	Hexane	~10[a]	-	-	-
PASPD-IO	H_2O	~50[a]	71.2[b]	0.017[c]	-
FA-PASPD-IO	H_2O	~50[a]	74.8[b]	0.016[c]	-
Gd-DTPA-PASPD-IO	H_2O	~50[a]	80.6[b]	0.017[c]	0.004[d]
Gd-DTPA-FA-PASPD-IO	H_2O	~50[a]	82.3[b]	0.016[c]	0.004[d]

[a] The diameter determined via TEM. [b] The diameter determined via DLS. [c] The Fe content determined via TGA. [d] The Gd content determined via ICP

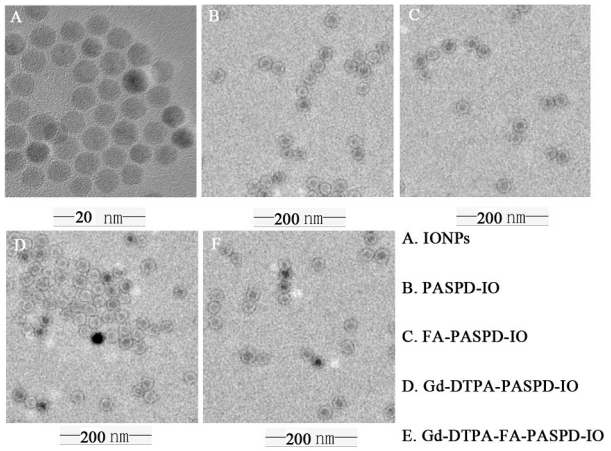

Fig. 1 TEM images of (A) IONPs (B) PASPD-IO (C) FA-PASPD-IO (D) Gd-DTPA-PASPD-IO (E) Gd-DTPA-FA-PASPD-IO

temperature with measuring the hydrodynamic diameters at a definite time interval.

Cytotoxicity assay

Cytotoxicity of NPs against HepG2 cells were measured by MTT assay. Experiments were conducted in triplicate. The cells were plated in 96-well plates (2×10^4 cells/well), maintained in 100 μL RPMI 1640 medium supplemented with 10% FBS and incubated for 24 h at 37 ℃ in a humidified atmosphere with 5% CO_2. After preincubation, the NPs with pre-defined concentrations ranged from 0.01 mg/mL to 0.5 mg/mL were added into the cell culture medium. After 24 h incubation, 20 μL of MTT (5 mg/mL in PBS) was added to each well and cells were incubated at 37 ℃. After an incubation period of 4 h, the medium was removed and the blue formazan crystals formed inside the cells were dissolved in 100 μL of DMSO. The absorbance was measured in a BioTek Elx 800 at a wavelength of 490 nm.

MRI in vitro

The targeting conjugate@IONPs with various iron concentrations were suspended in 0.5 mL tubes. The tubes were embedded in a home-made tank, which was designed to fit the MRI coil. T_1 and T_2-weighted MRI images were acquired on the MR scanner above with the following parameters: TR 3000 ms; TE 8, 10, 20, 40, 80, 100, 120, 140 ms, slice thickness 1 mm.

Stability of the dual-MR probe

To evaluate the stability of the NPs here, the NPs (0.2 mL, 10 mg/mL) were incubated in PBS buffer (2 mL, 1×) at room

MRI in vivo

The experimental protocol was approved by the Animal Studies committee of the Jilin University. For MR imaging, ICR male mice (6-7 weeks) were implanted with HepG2 cells (1×10^6 cells) by subcutaneous injection. When the tumors had grown to a volume of 200-500 mm^3, MRI experiments were did according to the method reported by Lee et al.[22] Briefly, MR images were taken prior to injection of NPs and at appropriate intervals post-injection. Mice received general drug anaesthesia. 0.2 mL dual-contrast (0.004 mmol Gd/mL, 0.028 mmol Gd/kg, 0.016 mmol Fe/mL, 0.110 mmol Fe/kg) was injected through the tail vein. MRI was performed using a 1.5 T Siemens Avanto MR scanner and an animal coil. All MRI quantitative analyses were carried out by on radiologist. The MRI images were exported as colour maps for investigating and evaluating more easily. Furthermore, In order to achieve quantitative analysis, a statistical study was investigated to exactly calculate the size of the colour region in the tumor site.

Results and discussion

Synthesis and characterization of PASPD

The synthetic route for the FA-PASPD is illustrated in Scheme 1. The detailed experiments are described in the supporting information. FA-PEG-NH_2 was initially prepared by activating the γ-carboxyl group in folic acid with EDC/NHS for the conjugation to primary amine groups of PEG-diamine. And then, PASP-g-(PEG-FA)-DDA-EDA (FA-PASPD) was synthesized through ring-opening of PSI with FA-PEG-NH_2, DDA and EDA in DMF. To demonstrate tumor targeting property of FA, PASP-g-PEG-DDA-EDA was also synthesized according to our previous work for comparison.[21] As described in our previous work, the ^{1}H-NMR spectrum of PSI shows the signal for the methyne proton (-C**H**-) of the repeating succinimide unit (δ=5.3 ppm).[21] After the reaction of PSI with MeO-PEG_{2000}-NH_2, the ^{1}H-NMR spectrum of PSI-g-PEG shows the signal for methyne proton (-C**H**-) of the repeating succinimide unit after ring opening by PEG (δ=4.6 ppm). The typical signals of PEG also can be observed at 3.5 ppm. According to the ratio of the peak area at 4.6 ppm to that at 5.3 ppm, the molar percentage of ring-opened succinimide groups in PSI by MeO-PEG_{2000}-NH_2 is calculated to be 30%. Similarly, the molar percentage of ring-opened succinimide groups in PSI by FA-PEG-NH_2 is also

calculated to be 30% (Fig. S1A). The aromatic folate proton peaks could be observed at δ 6.8-8.6 ppm. After the reaction of DDA (30% mol ratio of succinimide units), as shown in Fig. S2B, the signals that originated from the dodecylamine units were observed at 0.88 and 1.25 ppm. From the ratio of the peak area at 4.6 ppm to that at 5.3 ppm, the molar percentage of ring opened succinimide groups in PSI by PEG and DDA is calculated to be 60%, suggesting that 30% molar percentage of the succinimide

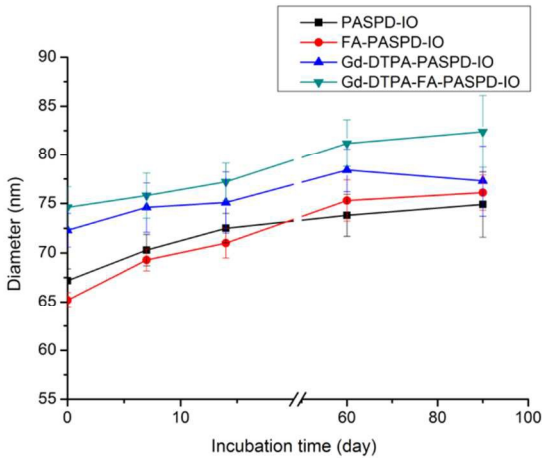

Fig. 2 The hydrodynamic diameters as a function of storage time at 4 ℃ for all the nanoparticles in PBS buffer (pH 7.4, 1×)

groups in PSI were opened by DDA. After the reaction of EDA, as shown in Fig. S1C, the signal for the methyne proton (-C**H**-) of the repeating succinimide unite at 5.3 ppm completely disappeared, indicating that all residual succinimide units had reacted with EDA. ^{1}H-NMR spectrum of PASP-g-PEG-DDA-EDA was also given in Fig. S1D for comparison.

Characterization of Gd-DTPA-FA-PASPD-IO

The synthetic mechanism of Gd-DTPA-FA-PASPD-IO was given in Scheme 2. The FA-PASPD which have hydrophilic segment (PEG) and hydrophobic segment (DDA) can be formed micelles easily. Hydrophobic-hydrophobic interaction between organic soluble IONPs and hydrophobic segments DDA of PASPD makes IONPs water-soluble. The surface amine groups of FA-PASPD-IO could be functionalized with DTPA, And then The DTPA-functionalized IONPs could load Gd^{3+} ions. TEM micrographs of the IO, FA-PASPD-IO, PASPD-IO, Gd-DTPA-FA-PASPD-IO and Gd-DTPA-PASPD-IO were shown in Fig. 1. The contents of IO in PASPD-IO and FA-PASP-IO were also measured by TGA analysis. The compound contained gadolinium as determined by elemental analysis. All the results were shown in Table 1.

Stability analysis

The stability in biological media is critical for contrast agent delivery system because the NPs should stay in the blood for enough long time for active recognition and being uptaken by the target organs. To evaluate the stability of the micelles here, it was incubated in PBS buffer (pH 7.4, 1×) at 37 ℃ with measuring the hydrodynamic diameters at a definite time interval. As shown in Fig 2, almost no change in the particles size was detected during 30 days storage time. The results indicated the high stability of the conjugate micelles in physiological conditions.

MTT analysis

The cytotoxicity in vitro of Gd-DTPA-PASPD@IO should been demonstrated because dual-contrast must show high biocompatibility. After 24 h incubation, the effect of dual-contrast with a series of concentrations on the viability of HepG2 cells was measured using the MTT assay. The cell viability results were shown in Fig. 3. None of the NPs with different

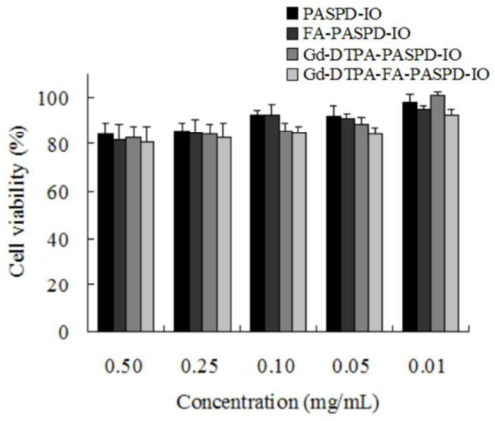

Fig. 3 Cytotoxicity of all the nanoparticles, the concentration range from 0.50 mg/mL to 0.01 mg/mL

concentration showed significant cytotoxicity against cells and 80% cells remained viable. The results suggested that the cytotoxicity of the dual-contrast was not affected by Gd-DTPA surface conjugating. Therefore, this dual-functional probe showed biocompatibility and potential applications of our nanoprobes for the imaging of cancers.

MRI in vitro

To evaluate the MRI contrast effect, a phantom study was performed with IONPs of elevated concentrations. As shown in Fig. 4A, the targeting IONPs displayed a clear concentration-dependent T_2 signal reduction effect, with a R_2 value of 173 $mM^{-1}s^{-1}$ (based on Fe concentration) This was likely attributed to a better magnetization control offered by no destroying of the surface of hydrophobic IONPs. The high R_2 values of the delivery system in comparison with commercially available products render them promising as an MRI-visible drug delivery system. To evaluate the T_1 reducing effect, the dual-contrast at different Fe concentrations above were investigated. Phantom images (Fig. 4B) demonstrated that T_1 signal intensity increased significantly compared with FA-PASPD-IO. The R_1 value of dual contrast was 40.2 $mM^{-1}s^{-1}$. Overall, the above results indicate that the indicate that the surface-conjugation of Gd-DTPA with the coating of IONPs showed no quenching of Gd.

MRI in vivo

T_1-weighted and T_2-weighted fast spin-echo images pre-, 0.5 h and 2 h post injection were acquired. As displayed in Fig. 5, a dramatic T_2 signal drop was witnessed at the tumor area after the

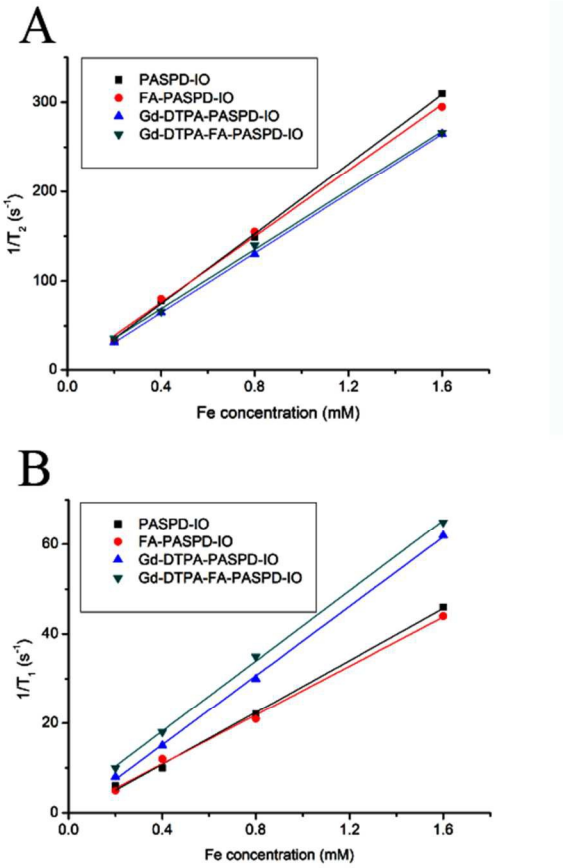

Fig. 4 (A) T_1-weighted images in vivo (B) T_2-weighted images in vivo

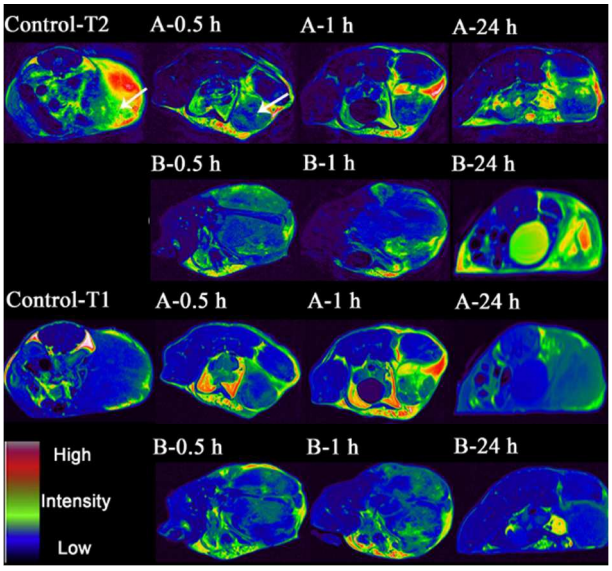

Fig. 5 T_2-weighted and T_1-weighted magnetic resonance images of tumor injected with (A) Gd-DTPA-FA-PASPD-IO and (B) Gd-DTPA-PASPD-IO. The arrows denote allograft tumors.

injection of FA-Gd-DTPA-IO-PASPD while a relative weak signal drop was observed in mice injected with Gd-DTPA-IO-PASPD. On the other hand, a dramatic T_1 signal increasement was witnessed at the tumor area after the injection of FA-Gd-DTPA-IO-PASPD while a relative weak signal increasement was observed in mice injected with Gd-DTPA-IO-PASPD. It is of note that even at the 24 h time point, the enhancement of FA-Gd-DTPA-IO-PASPD in dual-mode imaging was also observed compared with Gd-DTPA-IO-PASPD, suggesting a long circulation half-life of the FA-Gd-DTPA-IO-PASPD. As described above, the FA-Gd-DTPA-IO-PASPD could be used as a dual-mode imaging contrast with long circulation half-life. The half-life of Gd-DTPA was also prolonged.

Conclusions

In summary, a novel dual-MR contrast nanoprobe, based on Gd-DTPA surface conjugated SPIO nanomicelles was reported. The results demonstrated that the probe prepared this way could achieve T_1-weighted MR imaging and T_2-weighted MR imaging simultaneously, lengthen the half-life time, and make receptor-targeted internalization. Meanwhile the low cytotoxicity and high stability also proved that the nanoparticles could be used as a dual-MR probe from a practical standpoint. Overall, the FA-targeted Gd-DTPA surface conjugated SPIO nanomicelles could be a novel platform for cancer diagnosis technology.

Notes and references

[a] *Alan G. MacDiarmid Institute of Jilin University, 2699 Qianjin Street, Changchun, China. Fax: +86 0431 85168238; Tel: +86 0431 85168238; E-mail: liyapeng@jlu.edu.cn*

† Electronic Supplementary Information (ESI) available: [details of any supplementary information available should be included here]. See DOI: 10.1039/b000000x/

‡ Footnotes should appear here. These might include comments relevant to but not central to the matter under discussion, limited experimental and spectral data, and crystallographic data.

1 M. Rudin and R. Weissleder, *Drug Discov.*, 2003, **2**, 123
2 R. Hao,R. Xing,Z. Xu,Y. Hou,S. Gao,S. Sun, *Adv. Mater.*, 2010, **22**, 2729.
3 X. Kang, Z. Cheng, D. Yang, P. Ma, M. Shang, C. Peng, Y. Dai and J. Lin, *Adv. Mater.*,2012,**22**,1470.
4 X. Lu, R. Jiang, Q. Fan, L. Zhang, H. Zhang, M. Yang, Y. Ma, L. Wang and Wei Huang, *J. Mater. Chem.*, 2012, **22**, 6965
5 L. Frullano and T.J. Meade, *J. Biol. Inorg. Chem.*, 2007, **12**, 939
6 T. Chen, M.I. Shukoor, R. Wang, Z. Zhao, Q. Yuan, S. Bamrungsap, X. Xiong and W. Tan, *ACS Nano*, 2011, **5**, 7866
7 H.M. Kim, H. Lee, K.S. Hong, M.Y. Cho, M. H. Sung, H. Poo and Y.T. Lim, *ACS Nano*, 2011, **5**, 8230
8 T.P. Gazzi, L.A. Basso, D.S. Santos and P. Machado, *RSC Adv.*, 2014, **4**, 9880.
9 P. Mi, D. Kokuryo, H. Cabral, M. Kumagai, T. Nomotoa, I. Aoki,Terada, A. Kishimura, N. Nishiyama, K.Kataoka, *Journal of Controlled Release,*2014,**174**,63.
10 J. Hu , T. Liu , G. Zhang , F. Jin , S. Liu, *Macromol. Rapid Commun.* 2013, **34**, 749.
11 K.M. Bennett, J.Jo, H. Cabral, B.Rumiana, I.Aoki, Adv. *Drug Deliv. Rev.*, 2014, **74**,75.
12 H. Ishiwata, A. Vertut-Doi, T. Hirose and K. Miyajima, *Chem Pharm Bull (Tokyo)*, 1995, **43**, 1005
13 J.W. Bulte and D.L. Kraitchman, *NMR Biomed.*, 2004, **17**, 484
14 J. Zhuo and R.P. Gullapalli, *Radiographics*, 2006, **26**, 275
15 L. Macarini, S. Marini and P. Milillo, *Radiol Med.*, 2006, **111**, 1087
16 R.C. Semelka, J.K. Lee and S. Worawattanakul, *J. Magn. Reson. Imaging*, 1998, **8**, 670
17 J. Ward, J.A. Guthrie and D.J. Scott, *Radiology*, 2000, **216**, 154
18 N. Bolog, T. Pfammatter and B. Mullhaupt, *Abdom. Imaging*, 2008, **33**, 313
19 S. Santra, S.D. Jativa, C. Kaittanis, G. Normand, J. Grimm and J.M. Perez, *ACS Nano*, 2012, **6**, 7281
20 Y. Chang, N. Liu, L. Chen, X. Meng, Y. Liu, Y. Li and J. Wang, *J. Mater. Chem.*, 2012, **22**, 9594

21 H. Huang, Y. Li, X. Sun, Y. Lv, L. Chen and J. Wang, *New J. Chem.*, 2013, **37**, 1623.
22 Y. Lee, S.Y. Park, H. Mok and T.G. Park, *Bioconjugate Chem.*, 2008, **19**, 525.

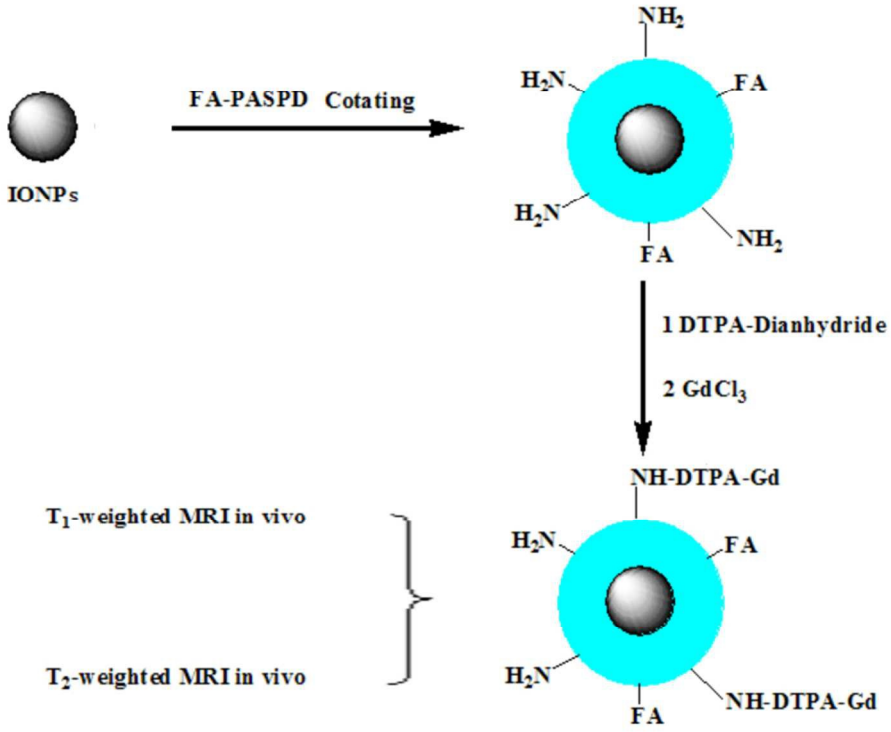

80x60mm (300 x 300 DPI)